Green Rooftop Analysis

Luca Bissoli - 257840
Dept. of Information Engineering and Computer Science
University of Trento
Trento, Italy
luca.bissoli@studenti.unitn.it

Alberto Messa - 258855
Dept. of Information Engineering and Computer Science
University of Trento
Trento, Italy
alberto.messa@studenti.unitn.it

***Abstract*—This work aims to compare two urban rooftop scenarios, cement roof and green roof, and to analyze how they interact with and modify the surrounding environment. The project focuses on building models capable of realistically simulating both micro-climate conditions and air pollution dynamics, using real-world datasets as inputs. We developed a physical model that integrates the dominant environmental processes, complemented in some cases by linear approximations guided by empirical constants. By feeding the physical model with data derived from the real datasets and performing a Monte Carlo analysis, we generated a sufficiently large set of simulations to confirm that green roofs exhibit beneficial properties: they contribute to milder temperatures and improved air quality for nearby buildings.**

I. Introduction

Green roofs have increasingly become a key component of urban sustainability strategies. These systems, which integrate vegetation layers on top of building rooftops, are now widely adopted across many cities as a response to rising temperatures, dense urbanization, and the need for more resilient infrastructure. Their growing popularity is supported by an extensive body of scientific and institutional research [1], [2], which highlights their ability to deliver multiple environmental and social benefits. Among the most documented advantages are stormwater retention, mitigation of the urban heat island effect, improved thermal performance of buildings, and support for urban biodiversity [3].

The influence of green roofs on microclimate is particularly relevant in dense urban environments. Vegetation and substrate layers reduce surface temperature through shading and evapotranspiration, thereby lowering heat transfer into buildings and contributing to cooler surrounding air [3]. Some studies also suggest that green roofs could contribute to air quality improvement by capturing certain airborne particulates, although the magnitude of this effect remains uncertain and highly dependent on local atmospheric conditions and roof design [1]. Beyond their environmental function, green roofs can enhance urban biodiversity, as demonstrated by large-scale adoption cases such as the city of Basel [4].

In this work, we focus on two closely related aspects: the potential attenuation of heat generated at roof level and the resulting impact on near-roof air quality. To address these questions, we needed to simulate the entire scenario from start to finish. Given the scalable nature of the project, we divided it into three distinct phases.

The first phase involved collecting real-world climatic and air-quality datasets, cleaning them, and using them to build models capable of generating realistic synthetic data. The second phase focused on constructing a physically based aerodynamics model which, using the meteorological and air-quality data as inputs, produced estimates of temperature reduction and pollutant mitigation. This model is not a precise replication of reality; since this phase falls outside the strict scope of the "Simulation and Performance Evaluation" course, we prioritized functionality over perfect realism.

The final phase concentrated on evaluation, where we applied the analytical and performance assessment tools introduced during the course to interpret the model outputs and compare the effects of green roofs versus conventional cement roofs.

II. Data Collection and Synthetic Data Modeling

To investigate the effects of green roofs, we first gathered and prepared environmental and air-quality data to build realistic synthetic datasets. We used *open-meteo.com*, a freely accessible platform providing historical meteorological data and air-quality measurements worldwide. For this study, we focused on the city of Rome, retrieving data from the past five years.

Two datasets were considered:

- **Meteorological dataset:** hourly temperature at 2m, wind speed at 10m, and shortwave radiation (W/m^2).
- **Air-quality dataset:** hourly measurements of carbon dioxide (ppm), PM10 ($\mu g/m^3$), PM2.5 ($\mu g/m^3$), and carbon monoxide ($\mu g/m^3$).

TABLE I: Overview of collected datasets for Rome (last 5 years).

Variable	Unit	Dataset
Temperature	°C	Meteorology
Wind Speed	m/s	Meteorology
Shortwave Radiation	W/m^2	Meteorology
Carbon Dioxide	ppm	Air Quality
PM10	$\mu g/m^3$	Air Quality
PM2.5	$\mu g/m^3$	Air Quality
Carbon Monoxide	$\mu g/m^3$	Air Quality

A. Trend Extraction and Residual Analysis

To generate realistic synthetic data, we first derived the deterministic *hourly trends* from the historical data. These trends represent the expected average value for each hour,

capturing daily patterns such as peak temperatures in the afternoon, typical diurnal wind behavior, and the absence of solar radiation at night.

Deviations from the trend, called *residuals*, reflect stochastic fluctuations not explained by the deterministic component. These residuals are modeled using Gaussian Mixture Models (GMMs) to account for multi-modal distributions observed in real data. The number of Gaussian components for each variable is selected based on the Bayesian Information Criterion (BIC), ensuring a balance between model complexity and fit quality.

The residuals are further characterized by their temporal autocorrelation and variability. Using the historical series, the AR(1) persistence parameter ϕ is calculated as the lag-1 autocorrelation of the residuals, while σ is derived as $\sqrt{1-\phi^2}$ to scale the stochastic innovation. The daily bias for each variable is estimated as the standard deviation of the daily means, capturing day-to-day variability. These parameters are then stored in tuning tables for use in the simulation phase.

B. Synthetic Data Generation

The synthetic data are generated by combining three components, each chosen to ensure both realism and interpretability:

1) **Deterministic trend:** the baseline hourly profiles. Preserving these trends ensures that the synthetic data reflect the observed seasonal and hourly dynamics.
2) **AR(1) stochastic residuals:** each residual r_t is modeled as

$$r_t = \phi\, r_{t-1} + \sigma\, \varepsilon_t,$$

where ϕ is the persistence parameter, σ scales the innovation, and ε_t is sampled from the fitted GMM. The AR(1) structure captures temporal autocorrelation, while the GMM allows multi-modal distributions and realistic deviations from the trend. Parameters ϕ and σ are derived directly from historical residuals, ensuring that the generated data maintain realistic temporal dynamics.
3) **Scenario-level bias:** a single daily perturbation drawn from a normal distribution simulates warmer/cooler or cloudier/clearer days. The standard deviation of daily means from historical data defines the magnitude of this bias, producing coherent daily scenarios.

Additional rules enforce physical consistency, such as setting radiation and residuals to zero at night or capping extreme temperature and wind values. This combination of deterministic trends, stochastic residuals with GMM innovations, and scenario-level bias produces synthetic data that maintain both temporal structure and realistic variability while being suitable for downstream modeling and evaluation.

C. Example of Data Processing

As an illustration, consider the temperature variable. Starting from the historical hourly trend, residuals are computed to capture stochastic deviations not explained by the deterministic pattern.

Before fitting a Gaussian Mixture Model (GMM), the optimal number of components is determined using the Bayesian Information Criterion (BIC). The BIC evaluates the trade-off between model complexity and goodness of fit: lower BIC values indicate a better balance. Figure 1 shows the BIC scores for different numbers of GMM components for temperature residuals. The number of components corresponding to the minimum BIC is selected for the GMM.

Figure 2 shows the histogram of residuals overlaid with the fitted GMM components, illustrating how the model reproduces the variability observed in the historical data.

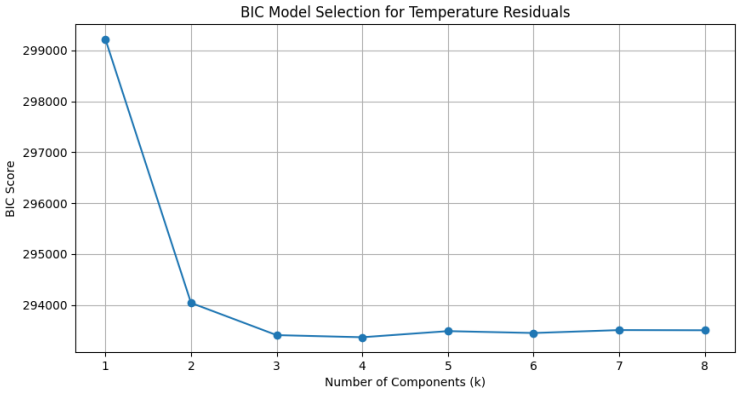

Fig. 1: BIC scores for different numbers of GMM components for temperature residuals. The optimal number of components corresponds to the minimum BIC.

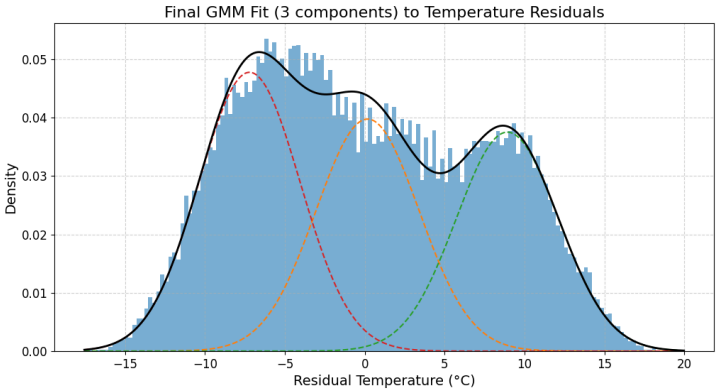

Fig. 2: Histogram of temperature residuals with fitted Gaussian Mixture Model.

This approach produces synthetic datasets suitable for feeding into the subsequent phases of our project, namely the physically-based modeling of building microclimate and air-quality evaluation.

III. Simulation Scenario and Conceptual Framework

This section outlines the conceptual logic behind the simulation. Rather than detailing the full thermodynamic derivations, which are available in the project repository[1], we focus here

[1]For the complete mathematical formulation and code implementation, please refer to the technical documentation in the project repository: https://github.com/bissochan/GreenRooftopAnalisys/blob/main/theory.md

on the simulation scenario, the core physical assumptions, and the logical flow of the model.

A. Simulation Scenario

The simulation is modeled as a simplified 2-D urban cross-section, designed to compare the microclimatic impact of a standard concrete roof versus a green roof. The geometry consists of three main elements arranged from left to right:

1) **Source Building (Left):** A lower building featuring the roof under analysis (Concrete or Green). This is the active surface where solar energy is absorbed and heat exchange occurs.
2) **Urban Gap:** A spatial separation between the two buildings where the air parcel travels and interacts with the environment.
3) **Target Facade (Right):** A taller adjacent building. This acts as the "receptor" where the impact of the heated air, specifically the buoyant plume rise, is evaluated.

The airflow is modeled horizontally from the source to the target. As the air passes over the source roof, it accumulates heat. Upon reaching the gap, it travels towards the facade, losing some heat to the environment due to mixing. The simulation concludes at the moment of impact with the target facade: here, the model records the final air temperature and calculates the potential buoyant plume rise (estimating the number of affected floors) and the final pollutant concentrations.

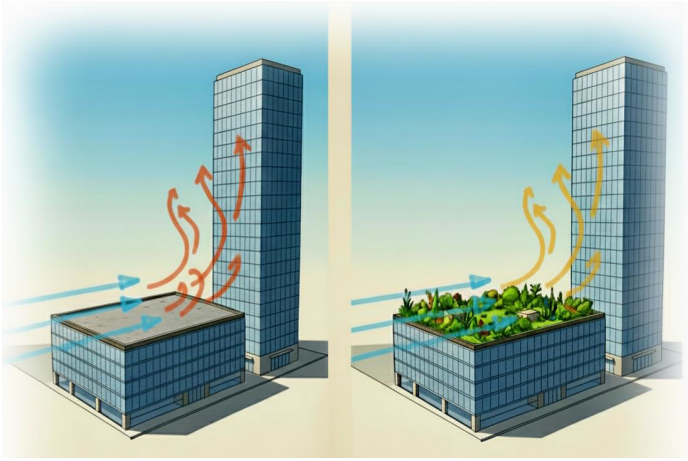

Fig. 3: Schematic comparison: the Concrete scenario (left) **would** generate intense convective heat (**red streamlines**), whereas the Green scenario (right) **should** produce a cooler airflow (**orange streamlines**) impacting the facade.

B. Key Assumptions

To balance physical realism with computational efficiency suitable for this study, the following simplifications were adopted:

- **2-D Geometry:** The model ignores lateral wind effects, assuming a uniform cross-section.
- **Convective Heating:** The air temperature increases strictly via convective heat transfer from the hot roof surface. Radiative trapping within the canyon is not modeled.
- **Eddy Mixing:** Turbulence is approximated using a simplified diffusivity parameter. We assume instantaneous vertical mixing, resulting in a **uniform temperature profile** (homogenized air) up to the calculated mixing height (H_{mix}).
- **Gated Rise during Transit:** Vertical displacement is calculated cumulatively while the air travels across the urban gap. This process is guided by a deterministic mathematical function. The simulation records the final height reached **at the moment of arrival** at the facade to determine the number of affected floors.

C. Physical and Ecological Logic

Thermo-Aerodynamic Logic: The thermal behavior is driven by the **Energy Balance** of the roof surface.

- **Concrete Scenario:** The roof heats up rapidly due to solar absorption. The only cooling mechanism is the transfer of heat to the air and the sky.
- **Green Roof Scenario:** The vegetation introduces a crucial cooling mechanism: *evapotranspiration*. Part of the incoming solar energy is used to evaporate water rather than heat the surface, resulting in lower surface temperatures.

As the wind pushes air over these surfaces, the air warms up. Since the green roof is cooler, the air passing over it gains less heat compared to the concrete roof. Consequently, when this air reaches the target facade, the "Green" air parcel has less buoyancy, potentially affecting fewer floors with waste heat compared to the "Concrete" parcel.

Ecological Logic: Beyond thermal regulation, the Green Roof model includes a module for ecosystem services, functioning as an active bio-filter:

- **Carbon Sequestration:** The vegetation absorbs CO_2 during daylight hours via photosynthesis, a process directly linked to the intensity of solar radiation.
- **Pollutant Removal:** The roof acts as a sink for particulate matter (PM10, PM2.5) and gases (CO). The model calculates the mass of pollutants removed via *dry deposition*, which depends on the concentration of pollutants in the air and the density of the vegetation (Leaf Area Index).

IV. Performance Evaluation Methodology

The evaluation framework relies on a dual-stage analysis strategy. First, we validate the synthetic input data to ensure statistical consistency with historical records. Second, we analyze the simulation outputs to quantify the physical and ecological differences between the Green and Concrete roof scenarios. This chapter details the datasets analyzed and the theoretical principles applied for validation and performance assessment.

A. Stage 1: Synthetic Data Validation (Input Analysis)

Before evaluating the physical model, it is mandatory to verify that the synthetic weather and air quality data generated by the stochastic engine (GMM + AR(1)) faithfully reproduce the statistical properties of the real historical observations.

Datasets Under Comparison: The validation process compares three distinct datasets for both meteorological (Temperature, Wind, Radiation) and air quality variables (CO_2, PM10, PM2.5, CO):

- **Historical Data (Real):** The raw observational data from Open-Meteo, serving as the ground truth.
- **Deterministic Trend:** The extracted hourly mean profiles representing the expected diurnal cycle.
- **Synthetic Samples (Simulated):** The output of the stochastic generator ($N = 5000$ runs), which includes random innovations and day-specific biases.

Statistical Validation Metrics: To assess the quality of the generation, the following statistical tests and visualizations are employed:

1) **Hourly Mean and Variability Analysis:** We compare the Hourly Mean and Standard Deviation of the synthetic data against the real data. A robust generator must preserve not just the average trend (bias ≈ 0) but also the natural fluctuations (volatility) of the phenomenon.
2) **Distribution Matching (ECDF & Q-Q Plots):** To verify that the Gaussian Mixture Models correctly captured the data distribution (including non-Gaussian tails), we analyze the Empirical Cumulative Distribution Functions (ECDF) and Quantile-Quantile (Q-Q) plots.
3) **Kolmogorov-Smirnov Test (KS Stat):** A quantitative non-parametric test is performed to measure the distance between the empirical distribution functions of the real and synthetic samples. A low KS statistic indicates that the synthetic data follows the same distribution as the real data.
4) **95% Confidence Intervals (CI):** Since the simulation is stochastic, we calculate the Confidence Intervals ($CI = \bar{x} \pm t \cdot \frac{s}{\sqrt{N}}$) around the synthetic means to verify if the real historical mean falls within the plausible range of the generated scenarios.

B. Validation Results: Synthetic Data Quality

Following the methodology outlined above, we analyzed the generated datasets. The validation highlights a generally high fidelity in reproducing the historical statistical properties, with specific deviations arising from necessary physical constraints imposed on the model.

1) Effective Simulation: Temperature: Temperature represents a robust example of the data generation process. As illustrated in the following figures, the stochastic model captures the core behavior of the variable with satisfactory accuracy.

- **Mean Profile and Confidence Intervals:** Figure 4 shows that the simulated mean profile preserves the diurnal cycle perfectly. The real historical mean falls consistently within the 95% Confidence Interval, although it tends to hover near the upper bound of the interval.
- **Distributional Fit:** The Histogram (Figure 5) demonstrates a strong overlap between the real and synthetic densities. The Q-Q Plot (Figure 6) reveals that the synthetic data follows an almost perfect Normal distribution, closely adhering to the theoretical diagonal.
- **Standard Deviation:** A notable distinction appears in the Standard Deviation profile (Figure 7). While the simulated standard deviation follows a smooth and "guided" trajectory, due to the use of the AR(1) autoregressive process, the real data exhibits erratic hour-to-hour fluctuations. Crucially, however, the *magnitude* of the variability is correctly captured (ranging between $6.5°C$ and $8.0°C$), meaning the simulation introduces the correct amount of noise, even if less volatile in its temporal distribution. This smoothing effect is a consistent feature observed across all simulated variables in this study.

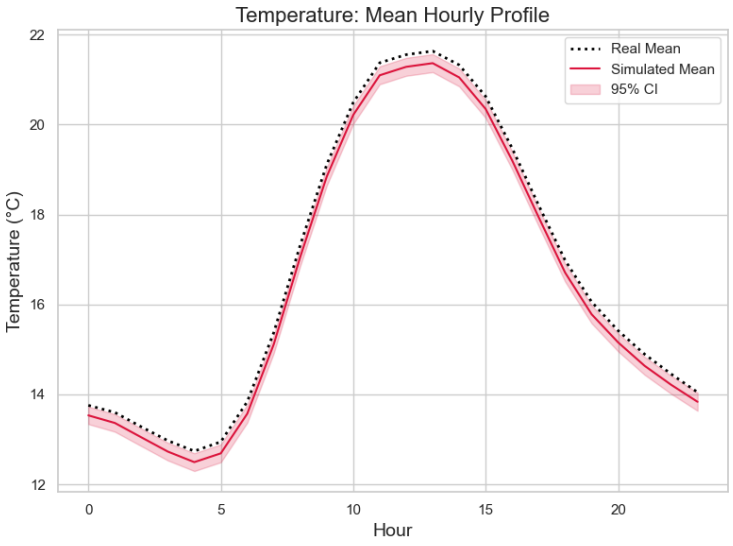

Fig. 4: Temperature: Hourly Mean Profile with 95% Confidence Interval.

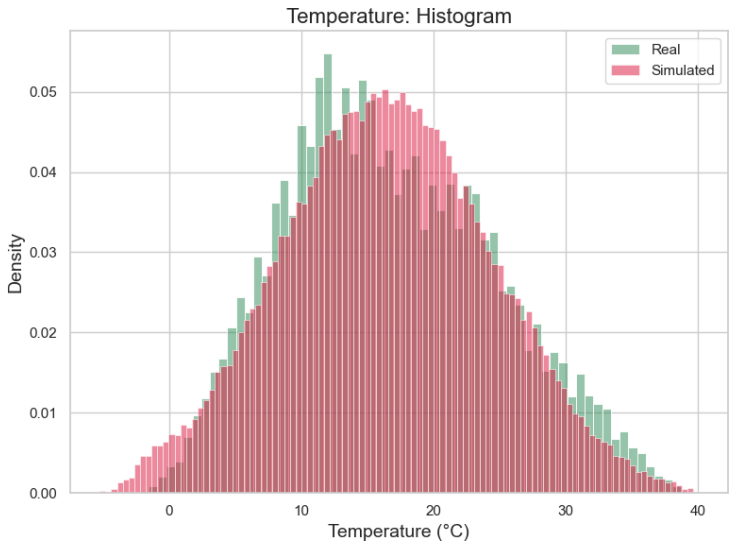

Fig. 5: Temperature: Probability Density Histogram showing excellent overlap.

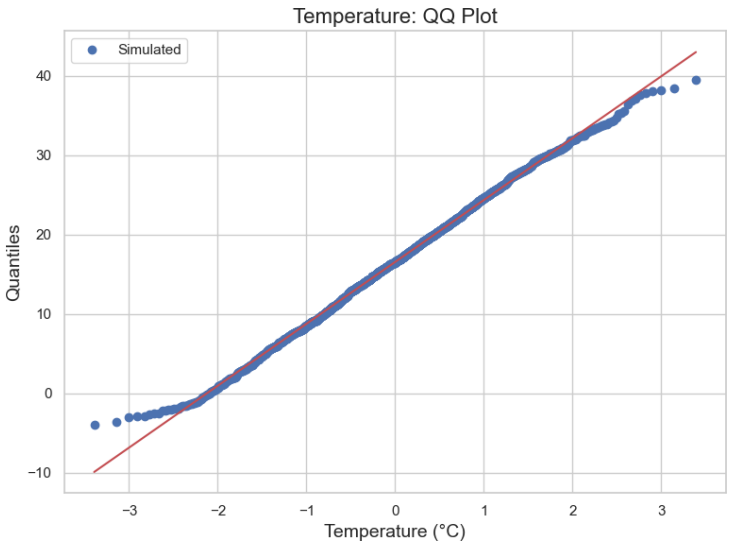

Fig. 6: Temperature: Q-Q Plot. The alignment with the diagonal indicates a near-perfect Normal distribution.

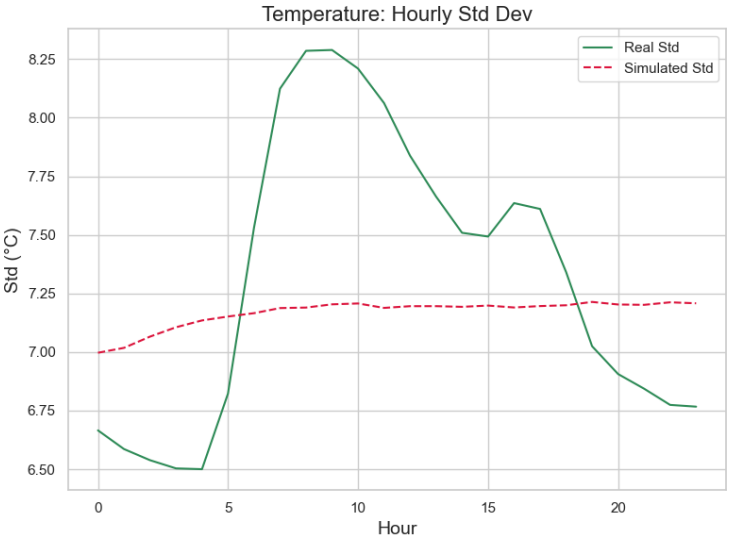

Fig. 7: Temperature: Hourly Standard Deviation comparison. The AR(1) process creates a smoother profile compared to real data.

2) Constrained Case: Wind Speed: The Wind Speed dataset presented a unique challenge requiring a trade-off between statistical fidelity and physical stability.

a) Physical Constraint (The 0.8 m/s Limit): During calibration, we observed that extremely low wind speeds caused numerical instabilities (overheating). To prevent this, a hard lower bound was applied: $\text{Wind}_{sim} = \max(\text{Wind}_{generated}, 0.8)$.

b) Statistical Consequences and Trade-offs: The imposition of the 0.8 m/s physical lower bound acts as a left-censoring of the wind distribution. This constraint introduces specific statistical artifacts that must be interpreted correctly:

- **Mean Shift:** The clamping effectively removes the lower tail of the distribution (values near zero), shifting the probability mass to the 0.8 m/s threshold. This results in an **artificial elevation of the simulated mean wind speed** compared to the historical record, as clearly visible in Figure 8.
- **Distributional Artifacts:** The Histogram (Figure 9) exhibits a pronounced density spike at 0.8 m/s, representing the accumulation of all low-wind events into a single bin. Consequently, the Q-Q Plot (Figure 10) shows a distinctive deviation in the bottom-left quadrant: while the theoretical Gaussian quantiles extend towards zero, the simulated sample quantiles hit a "floor" at 0.8, breaking the linearity of the Normal fit in the lower tail.
- **Overall Consistency vs. Stability:** Despite these local deviations, the ECDF (Figure 11) confirms that the general shape of the cumulative distribution remains valid for the majority of the domain. This confirms that the constraint successfully stabilizes the thermodynamic solver without compromising the statistical fidelity of medium and high wind speed scenarios.

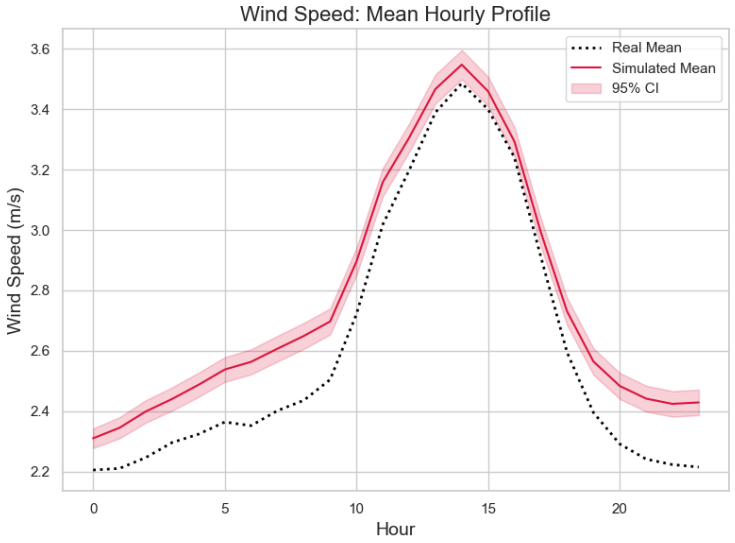

Fig. 8: Wind Speed: Hourly Mean Profile. The lower bound constraint slightly elevates the simulated mean.

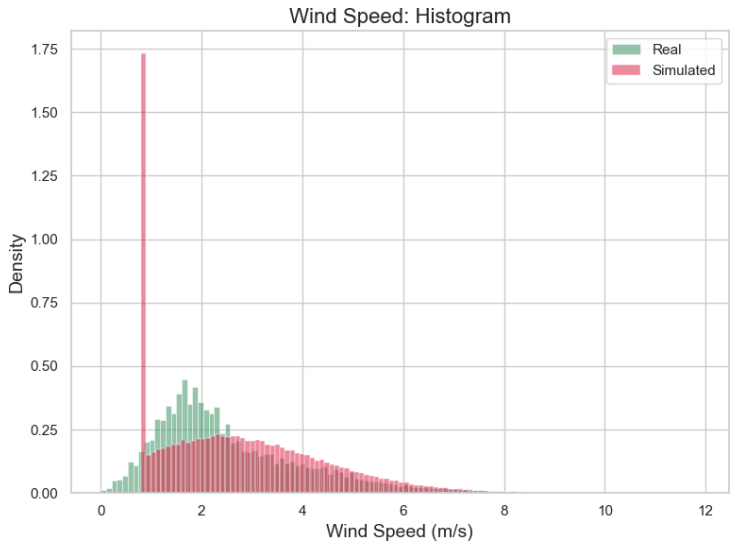

Fig. 9: Wind Speed: Histogram. Note the significant spike at 0.8 m/s due to the safety clamping.

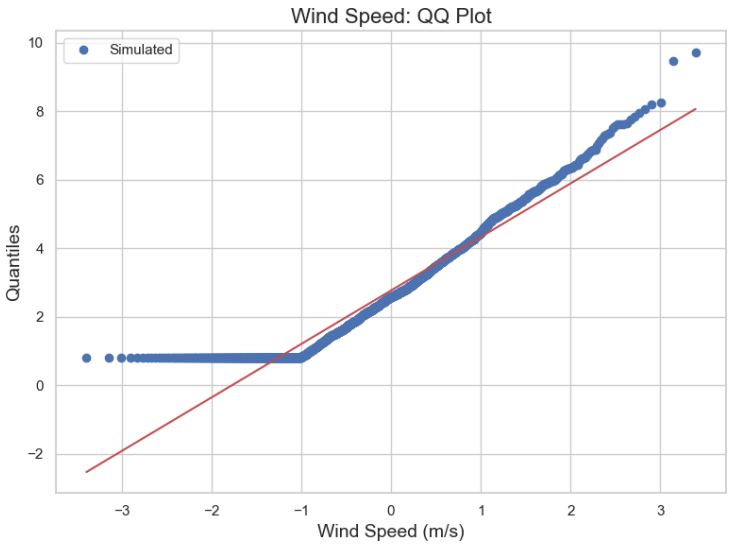

Fig. 10: Wind Speed: Q-Q Plot. The deviation at the bottom left reflects the artificial floor at 0.8 m/s.

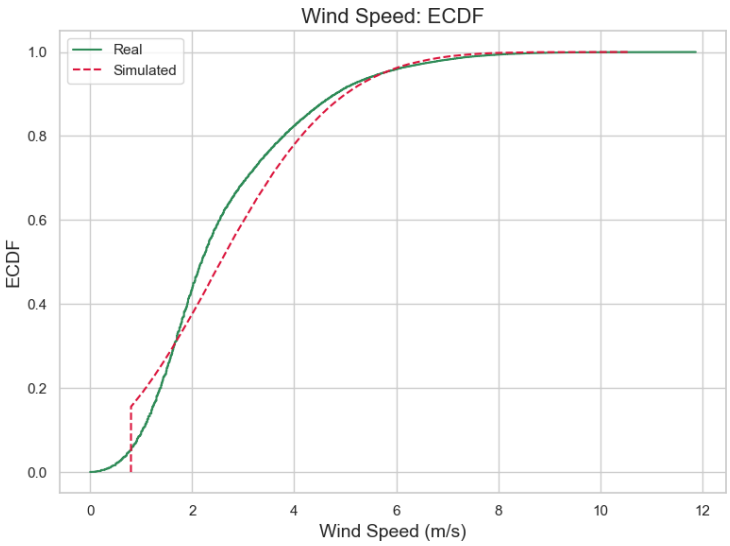

Fig. 11: Wind Speed: ECDF Comparison. The general distribution shape is preserved despite local artifacts.

3) Overall Assessment: In summary, the high fidelity observed for Temperature is representative of the general model behavior, extending to Solar Radiation and all Air Quality variables. Wind Speed constitutes the sole exception, where the deviation in the lower tail was an intentional and necessary trade-off to guarantee the thermodynamic stability of the simulation.

C. Stage 2: Simulation Output Analysis (Results)

The second stage focuses on the physical and ecological outputs generated by the Thermo-Aerodynamic model. The objective is to quantify the benefits of the Green Roof compared to the Concrete baseline and to assess the numerical stability of the simulation.

Datasets Analyzed: The analysis is performed on the Monte Carlo simulation results ('simulation_results.csv'), which contain hourly records for 5000 independent run iterations. The key variables analyzed are:

- **Thermal Variables:** Surface temperatures (T_{surf}), air temperature above the roof (T_{air}), and air temperature at the facade (T_{facade}) for both scenarios.
- **Aerodynamic Variables:** Mixing height (H_{mix}), Plume Rise, and the number of building floors affected.
- **Ecological Variables:** Mass of pollutants removed (PM10, PM2.5, CO) and Carbon sequestration.

Analysis Principles: The performance evaluation is grounded in the following analytical concepts:

1) **Monte Carlo Convergence:** To validate the reliability of the stochastic results, we analyze the cumulative mean of key variables (e.g., Green Roof Temperature) as a function of the accumulated hourly samples. Stability in the cumulative mean indicates that the total volume of generated data ($N = 5000$ runs $\times$ 24 hours) is sufficient to approximate the system's expected behavior.
2) **Comparative Delta Analysis:** We focus on the differential performance ($\Delta = \text{Cement} - \text{Green}$). This highlights the net benefit of the green infrastructure, specifically looking at the reduction in surface temperature and plume rise height.
3) **Range and Spike Checks:** Automated sanity checks are applied to ensure physical consistency, detecting unrealistic values (e.g., temperatures outside $[-20, 55]^\circ$C) or impossible hour-to-hour jumps (spikes), which would indicate numerical instability in the Euler integration.
4) **Uncertainty Quantification:** For every output metric (e.g., total CO_2 removed), we report not just the mean value but also the variance and percentiles (5th, 95th), providing a risk assessment of the green roof's performance under varying weather conditions.

D. Simulation Results: Physical Performance Analysis

Having validated the input data, we now evaluate the physical outputs of the model. The analysis relies on a total dataset of **120,000 hourly samples**, resulting from 5000 independent daily simulations. This provides a robust statistical basis for comparing the Concrete and Green roof scenarios.

1) Numerical Stability and Convergence: To verify the reliability of the stochastic simulation, we analyze the convergence of the **Green Roof Surface Temperature** (T_{green}). This variable serves as the primary stability indicator as it integrates all dynamic inputs (solar gain, convection, and evapotranspiration).

Figure 12 plots the cumulative running mean across the entire sample set. The profile exhibits initial volatility but achieves a stable equilibrium around **40,000 samples** (equivalent to approx. 1,666 simulated days). Since the simulation extends to 120,000 samples, this confirms that the chosen duration is more than sufficient to capture the system's expected behavior with high confidence.

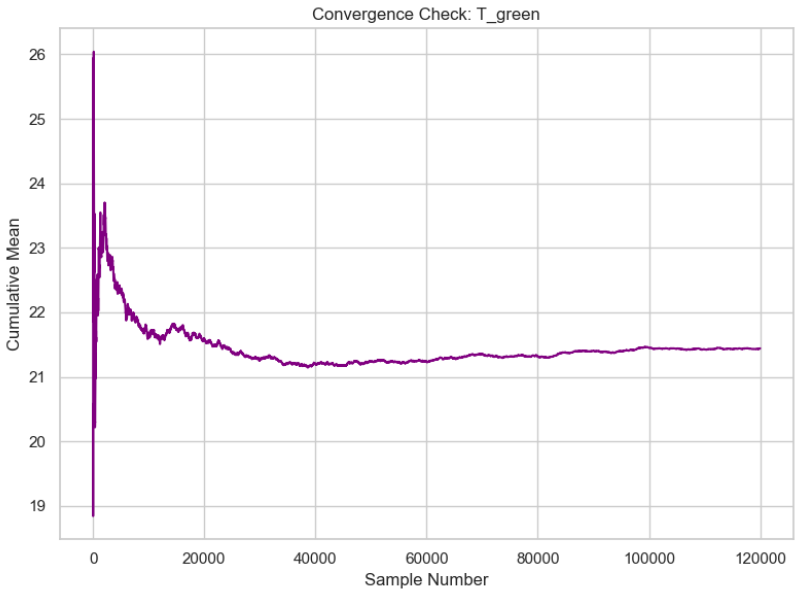

Fig. 12: Monte Carlo Convergence: The cumulative mean of the Green Roof temperature stabilizes after approximately 4000 samples.

2) Thermal Analysis and Comparative Benefits: This section analyzes the thermal evolution of the urban canyon. We first establish the baseline behavior using the standard Concrete scenario, and then quantify the specific cooling benefits provided by the Green Roof.

a) Thermal Propagation (Concrete Baseline): Figure 13 illustrates the damping effect as heat propagates from the surface to the facade in the standard scenario:

- **Surface (T_{surf}):** Exhibits extreme variability, with peaks exceeding $70°C$ due to direct solar absorption.
- **Air (T_{air}):** Convection moderates these extremes, with medians hovering around $30 - 35°C$ during peak hours.
- **Facade (T_{facade}):** Due to the thermal decay during transit across the urban gap, the temperature further relaxes towards ambient levels, reducing the thermal load on the adjacent building.

b) The "Green" Delta: Figure 14 quantifies the net benefit (Δ = Concrete − Green):

- **Surface Cooling:** The evapotranspiration effect is massive, reducing peak surface temperatures by $8 - 10°C$ on average.
- **Air Cooling (Roof):** This surface benefit translates into a $2.5°C$ reduction in the air temperature immediately above the roof.
- **Facade Air Cooling:** Crucially, this benefit propagates across the gap. The simulation shows that the air impacting the adjacent facade is consistently cooler (Fig. 14c), directly improving the thermal boundary condition for the neighboring building.

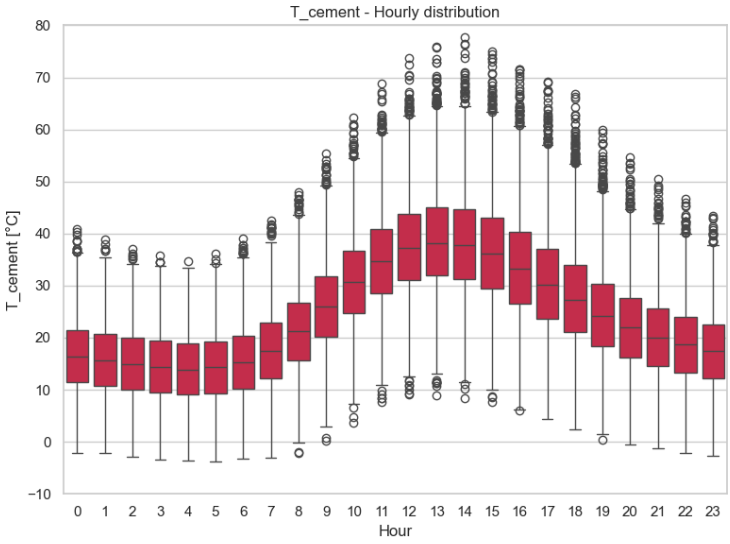

(a) Roof Surface Temperature (Extreme Heat)

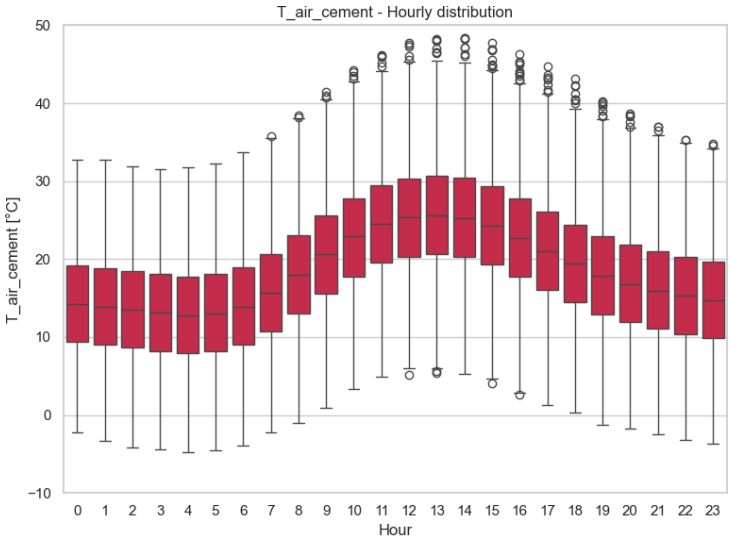

(b) Air Temperature Above Roof (Convective Transfer)

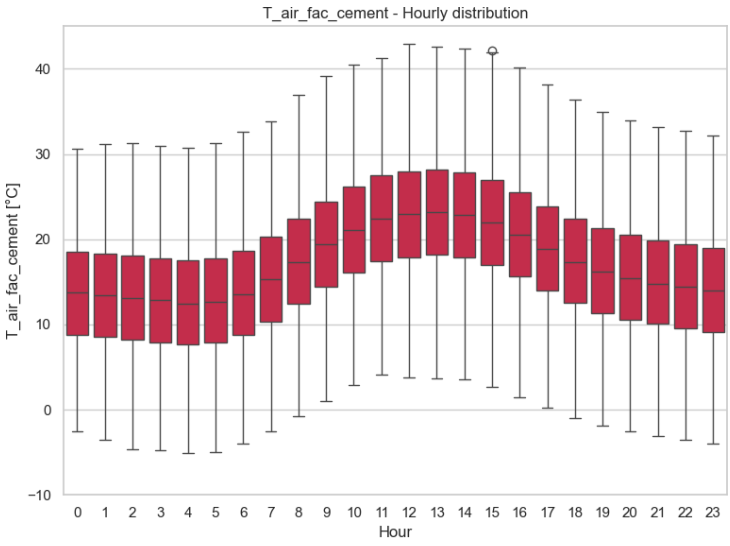

(c) Air Temperature at Facade (After Decay)

Fig. 13: Thermal Baseline (Concrete): Boxplots showing the propagation and attenuation of heat from the surface to the facade.

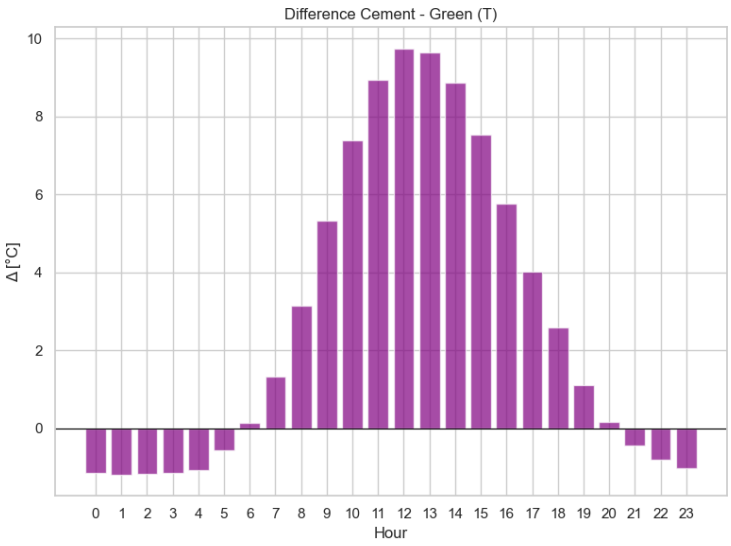

(a) Δ Surface Temp ($C - G$)

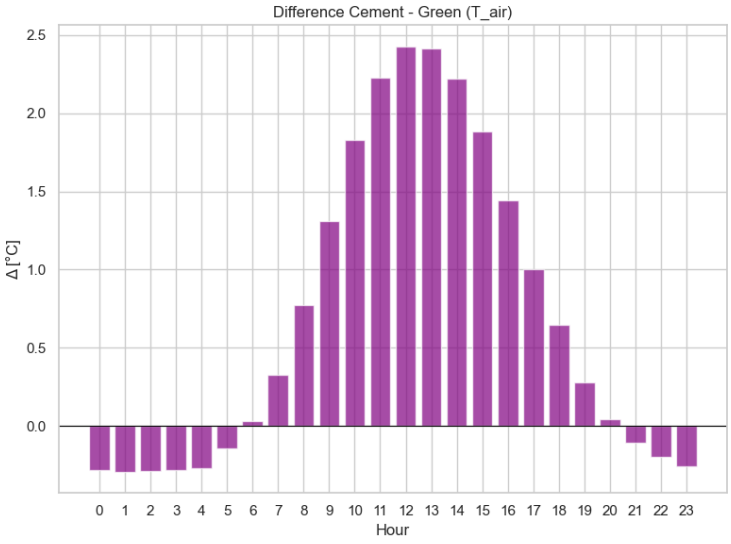

(b) Δ Air Temp (Roof)

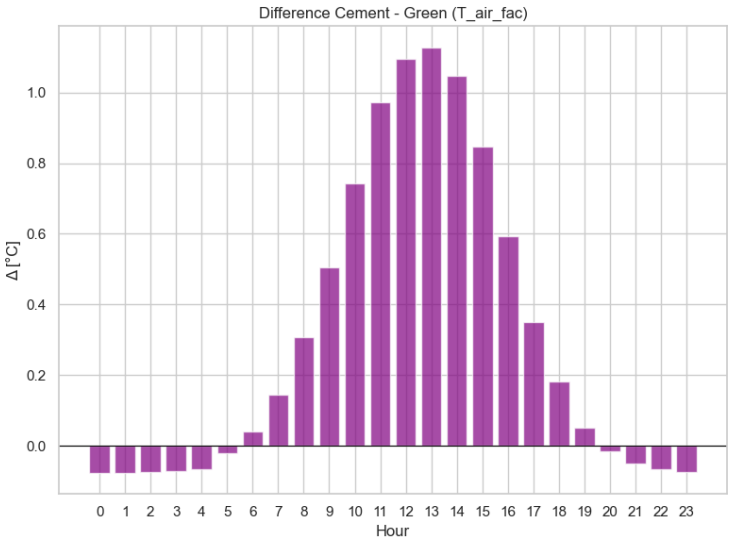

(c) Δ Facade Air Temp [°C]

Fig. 14: The "Green Delta": Positive values indicate how much hotter the Concrete scenario is compared to the Green one at different stages.

3) Architectural Impact: Affected Floors: Finally, we translate these thermodynamic variables into a metric relevant for urban design: the number of floors on the adjacent building impacted by the thermal plume.

Figure 15 compares the hourly distribution of affected floors.

- **Concrete Scenario:** Frequently impacts up to the **3rd floor** during peak hours (10:00 - 16:00).
- **Green Scenario:** Rarely exceeds the **2nd floor**, effectively sparing one full story of the adjacent building from the convective heat load.

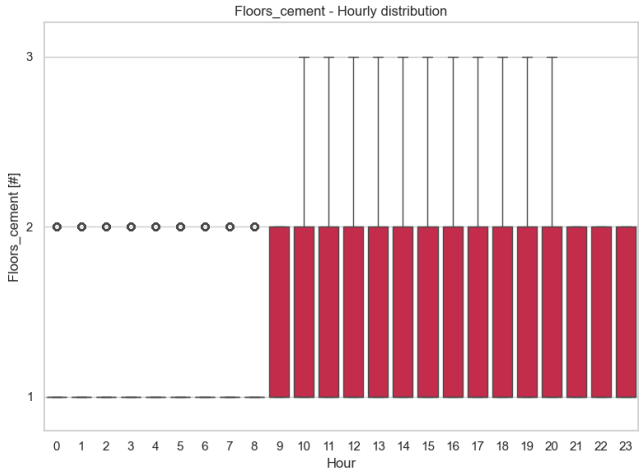

(a) Concrete: Impacts up to 3 floors.

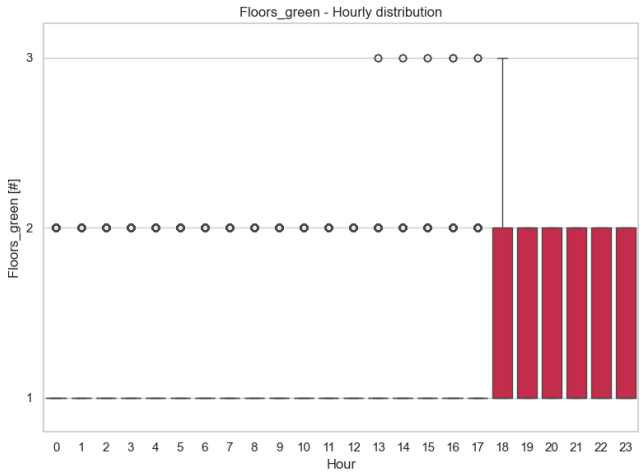

(b) Green: Contained within 2 floors.

Fig. 15: Architectural Impact: Comparison of building floors affected by the buoyant thermal plume.

a) Ecological Performance: Pollution Removal Across Temporal Scales: The green roof model incorporates pollutant removal mechanisms beyond thermal mitigation, enabling a multi-metrical performance evaluation. The Monte Carlo simulation (5000 runs) quantifies removal efficacy across CO_2, CO, PM_{10}, and $PM_{2.5}$, revealing distinct behavioral patterns (Figure 16).

b) Ecological Performance: Pollution Removal Across Temporal Scales: The green roof model incorporates pollutant removal mechanisms beyond thermal mitigation, enabling a multi-metrical performance evaluation. The Monte Carlo simulation (5000 runs) quantifies removal efficacy across CO_2, CO, PM_{10}, and $PM_{2.5}$, revealing distinct behavioral patterns (Figure 16).

While CO_2 uptake provides a measurable contribution governed by photosynthetic processes coupled to solar radiation—yielding predictable diurnal patterns with low variance—particulate matter (PM_{10}, $PM_{2.5}$) exhibits constant $\sim 5\%$ removal rates across all hours. This uniformity stems from the ventilation model: removal percentage = airflow/column volume, independent of concentration [5], [7].

The consistent particulate reduction (CO: 5.2%, PM10: 5.1%, PM2.5: 5.3%) contrasts sharply with CO_2's variable uptake, highlighting the green roof's dual-mode operation: *radiation-coupled photosynthesis + wind-coupled filtration*. This asymmetry reveals critical insights:

- *Predictability:* CO_2 removal is solar-driven (highly predictable); PM removal is wind-driven (stochastic but consistently effective).
- *Performance:* Despite equivalent % removal, particulates represent higher absolute mass reduction due to elevated concentrations.
- *Robustness:* Ensemble averaging smooths wind variability, yielding reliable daily PM mitigation ($\sim$5% reduction, 24/7).

Thus, the ecological module demonstrates multidimensional performance: predictable CO_2 sequestration paired with robust, constant particulate filtration—making green roofs reliable urban pollution control systems [1], [5].

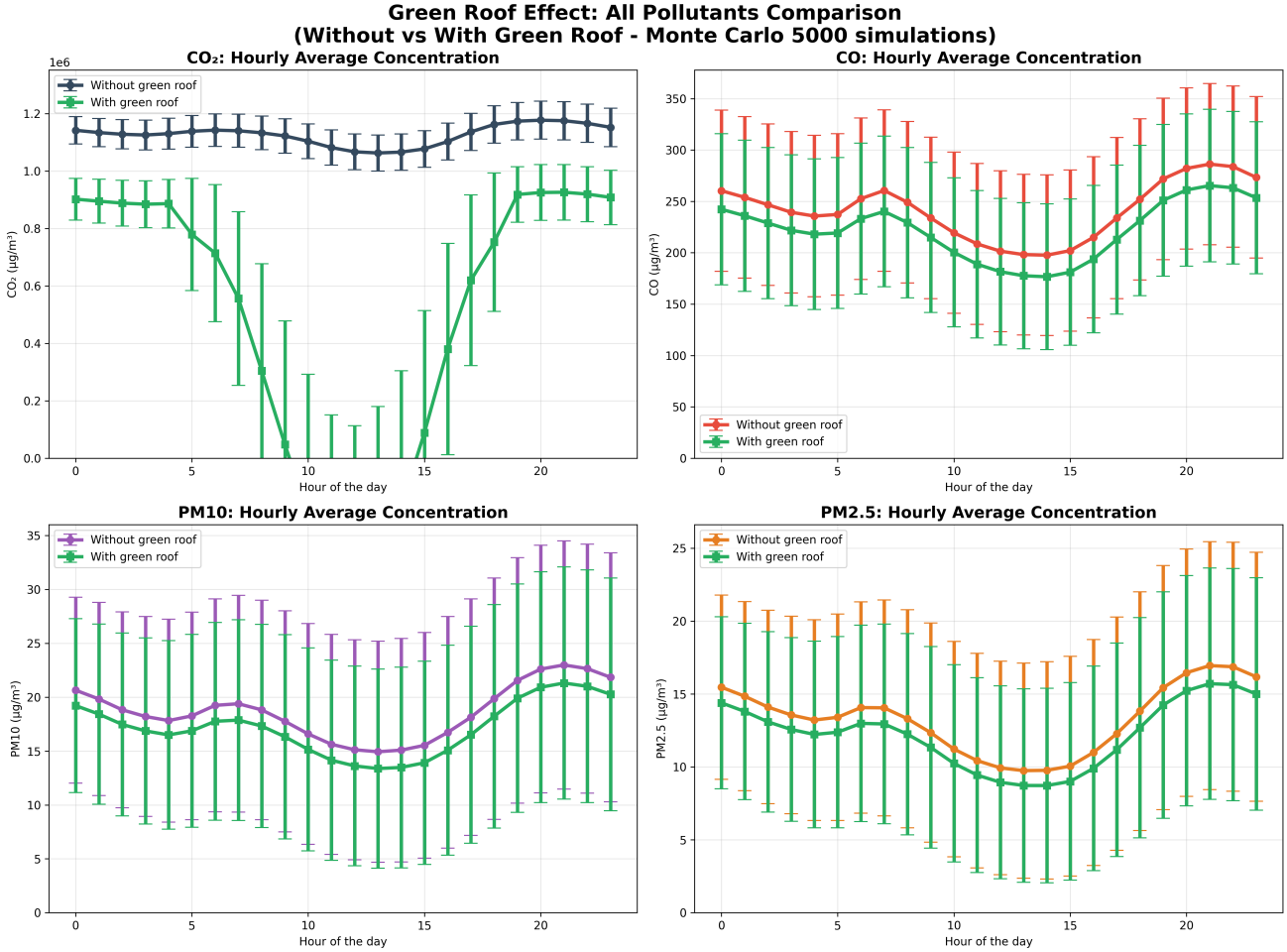

Fig. 16: Hourly average pollutant concentrations: without (solid lines) vs with green roof (dashed lines). Error bands show $\pm 1\sigma$ from Monte Carlo ensemble (5000 simulations). Particulates show consistent $\sim 5\%$ reduction driven by wind-dependent ventilation; CO_2 exhibits diurnal photosynthetic peak.

V. Conclusion

This project provided an opportunity to combine multiple concepts introduced during the course, with a particular focus on stochastic modeling and performance evaluation. While the physical and ecological mechanisms were simplified, the main effort was devoted to building a statistically consistent synthetic dataset, ensuring reproducibility of environmental patterns, and integrating it into a full simulation pipeline. Developing the models required addressing several practical challenges along the way, from data cleaning and parameter tuning to designing a coherent simulation framework, which proved useful for gaining familiarity with real-world problem solving.

Working through these stages highlighted a key distinction between studying a concept in theory and applying it within a complete system: theoretical knowledge provides the foundation, but building a functional model requires iterative refinement, assumptions management, and systematic validation. Overall, the project was a valuable learning experience that allowed us to consolidate the statistical and methodological tools of the course while experimenting with their application in a simplified environmental scenario.

References

[1] Nguyen C.N., Muttil N., Tariq M.A.U.R., and Ng A.W.M., "Quantifying the Benefits and Ecosystem Services Provided by Green Roofs: A Systematic Review," *Water*, vol. 14, no. 1, p. 68, 2022. [Online]. Available: https://www.mdpi.com/2073-4441/14/1/68

[2] European Commission, BUILD UP, "Long-term Benefits of Green Roofs and Facades – In-depth Analysis," 2024. [Online]. Available: https://build-up.ec.europa.eu/en/resources-and-tools/publications/long-term-benefits-green-roofs-and-facades-depth-analysis

[3] US Environmental Protection Agency, "Using Green Roofs to Reduce Heat Islands," 2025. [Online]. Available: https://www.epa.gov/heatislands/using-green-roofs-reduce-heat-islands

[4] The Guardian, "'Green roofs deliver for biodiversity': how Basel put nature on top," 2025. [Online]. Available: https://www.theguardian.com/environment/2025/feb/28/green-roofs-deliver-for-biodiversity-how-basel-put-nature-on-top

[5] American Society of Landscape Architects (ASLA), "Green Roofs and Air Quality," 2020. [Online]. Available: https://www.asla.org/greenroofeducation/cleantheair.html

[6] U.S. National Park Service, "How Trees Clean the Air," 2021. [Online]. Available: https://www.nps.gov/articles/000/uerla-trees-air-pollution.htm

[7] International Association of Horticultural Producers (AIPH), "Vegetation as an Urban Air Filter," 2022. [Online]. Available: https://aiph.org/green-city/guidelines/green-city/green-city-filtering/